Institute of Aerodynamics and Chair of Fluid Mechanics

RWTH AACHEN UNIVERSITY

**Diese Arbeit wurde vorgelegt am Aerodynamischen Institut**

# Investigations on two-way coupling effects of particle-laden decaying isotropic turbulent flows

---


Projektarbeit

von

Julian Stemmermann, Steffen Trienekens

und Christian Soika

Aerodynamisches Institut der RWTH Aachen


September 23, 2017


Betreuer: Konstantin Fröhlich

Erstprüfer: Univ.-Prof. Dr.-Ing. Wolfgang Schröder

# Contents

# 1 Nomenclature

| | |
|---|---|
| $\eta$ | Kolomogorov scale |
| $\boldsymbol{\tau}$ | Stress tensor |
| $\boldsymbol{I}$ | Identity tensor |
| $\boldsymbol{S}$ | Rate-of-strain-tensor |
| $\mu$ | Dynamic viscosity |
| $\rho$ | Density |
| $\rho_\mathrm{p}$ | Particle density |
| $\tau_m athrmp$ | Particle response time |
| $\boldsymbol{\nabla}$ | Nabla-operator |
| $\boldsymbol{a}$ | particle acceleration |
| $\boldsymbol{H}^\mathbf{i}$ | Stores the inviscid variables in the flux-vector included in the Navier-Stokes equations |
| $\boldsymbol{H}^\mathbf{v}$ | Stores the viscous variables in the flux-vector included in the Navier-Stokes equations |
| $\boldsymbol{H}$ | Container for fluctuating variables in the Navier-Stokes equations |
| $\boldsymbol{Q}$ | Container for conserved variables in the Navier-Stokes equations |
| $\boldsymbol{q}$ | Heat conduction |
| $\boldsymbol{u}$ | Three-dimensional velocity |
| $\boldsymbol{v}_\mathbf{p}$ | Particle velocity |
| $\boldsymbol{v}$ | particle velocity |
| $\boldsymbol{x}_\mathbf{p}$ | Particle position |
| $\boldsymbol{x}$ | particle position |
| $c_p$ | Specific isobaric heat capacity |
| $c_v$ | Specific isochoric heat capacity |
| $E$ | Specific inner energy |
| $e$ | Specific internal energy |
| $f_m athrmD$ | Drag correction |
| $k_t$ | thermal conductivity |
| $m_\mathrm{c}$ | number of clustered particles |
| $p$ | Pressure |
| $Pr$ | Prandtl number |
| $R$ | Universal gas constant |
| $r_p$ | Particle radius |
| $Re$ | Reynolds number |
| $S$ | Sutherland temperature |
| $T$ | Temperature |

# 2 Introduction

This paper deals with the effects of particles on an the flow conditions of isotropic turbulent flows. There are many examples of these particle laden turbulent flows in nature, for example in volcanic eruptions and in the "white water" of breaking waves.

Multiphase flows also occur in technical applications. Spray automization in fuel injectors, cyclonic particle separation in oil rafinery and sediment accumulation in pipelines are just three of many cases, where it is of huge interest to predict the influence of particles on the turubulence of the mean flow. Of major industrial interest is the fuel dispersion and the combustion of the dispersed fuel in the combustion chamber. To get a homogeneous and fast combustion, both should take place at turbulent flow conditions. So it is an important question, in which way and intense the particles influence the turbulence.

Another important example is an fluidized bed. This is an application to realize an effective suspension and combustion of fluid particles in a vessel. The particles, which are at the bottom of the vessel, are suspended by a fluid, in most cases a gas, that streams from beyond the particles threw the porous bottom, if the pressure is larger than the gravitiy of the particles. While this happens the fluid suspends the particles and the contact between fluid and particles is very intimate, which fascilates for example the combustion of material with a low caloric content, the in situ absorption of the pollutants deriving from the combustion and the action of a catalyst. This process aims to produce a suspension with less heterogeneous regions, what means bubbles with a much smaller concentration of particles. Hence turbulence is very important requirement to produce a homogeneous fluid stream for effective and complete combustion.

In this work the influence of the particles on the streaming conditions is presented by using DNS and LES simulations. The focus lies on analyzing the energy transfer between particles and fluid as well as the intensity of the decrease of turbulent kinetic energy in the fluid. At the begining some mathematical background information about modeling turbulent single phase and particle laden flows are given. Here the Navier Stokes equations and the Kolmogorov scales are presented as an approach to model turbulence. In addition to this for particle laden flows the equations of motion are expanded by a new term that desribes the forces acting between fluid and particles. Also the coupling rate, that describes the exchanged energy is introduced. Then the computational basics of methods used in this work are introduced. First the simulation methods DNS and LES, how they work and in which case which one is used is explained. Them the used discretization tool to

integrate the particle tracking equartions, that works with a predictor-corrector-scheme, is described. Finally the computational method 'particle clustering' is introduced. This approach aims to decrease the computational effort of particle laden simulations. It works that way that the particles are coupled to cluster and each cluster is considered as one particle.
In the following the deviations caused by using this method are determined and the applicability is evaluated. Therefore the influence of the number of particles per cluster on the accuracy of the plots of the turbulent kintic energy and the exchanged energy beween particles and fluid per time is identified. Also the number of particles that is needed to get consistent average values for the flow characteristics is investigated.

# 3 Mathematical models

## 3.1 Single-phase flow

In this section the mathematical basics for understanding and simulating turbulent flows are discussed. However, it should be pointed out that this is no complete treatise of the mathematical and physical basics. The reader can achieve further insight on this topic by looking at different books and papers, e.g. [**?**].

### 3.1.1 The Navier-Stokes equations

The Navier-Stokes-Equations are of great importance for understanding turbulent phenomena. This set of equations exists in forms for compressible and incompressible fluids. For an infinitesimal small volume element $\mathrm{d}\tau$ and using the cartesian coordinate system, they can be written in the so-called 'divergence form':

$$\frac{\partial \boldsymbol{Q}}{\partial t} + \boldsymbol{\nabla} \boldsymbol{H} = 0 \tag{3.1}$$

The vector $\boldsymbol{Q}$ contains all the variables which are conserved, i.e. the density $\rho$, the velocity $\boldsymbol{u}$ and the specific inner energy $E$:

$$\boldsymbol{Q} = \begin{pmatrix} \rho \\ \rho \boldsymbol{u} \\ \rho E \end{pmatrix} \tag{3.2}$$

$\boldsymbol{H}$ is the flux vector which stores all the floating variables and may be split up into two parts:

$$\boldsymbol{H} = \boldsymbol{H}^{\mathbf{i}} + \boldsymbol{H}^{\mathbf{v}} \tag{3.3}$$

The contents of the two vectors are displayed below:

$$\boldsymbol{H}^{\mathbf{i}} = \begin{pmatrix} \rho \boldsymbol{u} \\ \rho \boldsymbol{u}\boldsymbol{u} + p \\ \boldsymbol{u}(\rho E + p) \end{pmatrix} \tag{3.4}$$

$$\boldsymbol{H}^{\mathbf{v}} = -\frac{1}{Re} \begin{pmatrix} 0 \\ \boldsymbol{\tau} \\ \boldsymbol{\tau}\boldsymbol{u} + \boldsymbol{q} \end{pmatrix} \tag{3.5}$$

$\boldsymbol{H}^{\mathbf{i}}$ is called inviscid flux and contains only the variables that are independent of the fluids viscosity, it describes the way a fluid with zero viscosity would behave. In contrast, the viscous flux $\boldsymbol{H}^{\mathbf{v}}$ represents the effects of viscosity. The Reynolds

number $Re = \frac{\rho v d}{\eta}$ is defined to be the ratio of inertia to tenacity, which makes it very valuable for understanding turbulent flows. This is also due to the fact that two familiar objects with the same Reynolds number behave similar in turbulence. One can assume that flows with $Re << 1$ are laminar and flows with $Re >> 1$ are turbulent. To solve the Navier-Stokes-Equations, more information regarding some variables is required. For Calculating the specific inner Energy $E$ and the heat conduction $\boldsymbol{q}$, the following equations are used:

$$E = e\frac{1}{2}|\boldsymbol{u}|^2 \tag{3.6}$$

$$\boldsymbol{q} = -\frac{\mu}{Pr(\gamma - 1)}\boldsymbol{\nabla} T \tag{3.7}$$

with

$$\gamma = \frac{c_p}{c_v} \tag{3.8}$$

and the Prandtl number

$$Pr = \frac{\mu_\infty c_p}{k_t} \tag{3.9}$$

using the specific heat capacities of the fluid $c_v$ and $c_p$. If one could assume that the fluid is a newtonian fluid, the linear correlation between stress and the rate of strain results in:

$$\boldsymbol{\tau} = 2\mu\boldsymbol{S} - \frac{2}{3}\mu(\boldsymbol{\nabla} * \boldsymbol{u})\boldsymbol{I} \tag{3.10}$$

in which $\boldsymbol{S} = \frac{(\boldsymbol{\nabla u})(\boldsymbol{\nabla u})^T}{2}$ denotes the rate-of-strain-tensor. Additionally, the viscosity $\mu$ can be aprroximated through Sutherland's law, which is based on the ideal gas-theory:

$$\mu(T) = \mu_\infty \left(\frac{T}{t_\infty}\right)^{3/2} \frac{T_\infty + S}{T + S} \tag{3.11}$$

S is in this case the Sutherland temperature. To achieve closure the caloric state equation $e = c_v T$ and the state eqaution for an ideal gas $p = \rho R T$ are used. The specific gas constant is determined by $R = c_p - c_v$. These equations form a set of partial differential equations, so for solving them starting values are needed.

### 3.1.2 Turbulent motion across all scales

Turbulent flows contain eddies of all sizes and forms. Large-scale eddies bring energy to the flow which is then passed down to smaller-scale eddies and in the end dissipated into heat by viscous effects. This behavior is called the 'energy cascade' and was first described by Richardson in the year 1922. The theory then was developed further by Kolmogorov and published 1941.
The first set of scales describe the large eddies. These scales are called *integral* scales and are determined by the physical boundaries of the flow. As said before, at these scales the energy is brought into the flow, creating the so-called 'energy-containing range'. The length scale is the called integral length scale $L$, and the corresponding timescale which is most times called 'eddy turnover time' is defined as:

$$\tau_{\mathrm{L}} = \frac{L}{U} \tag{3.12}$$

where $U$ denotes the characteristic velocity.
The smallest scales in a turbulent flow are the Kolmogorov length ($\eta$) and time ($\tau_\eta$) scale. At this scales, the effects of viscosity take place and the energy dissipates into heat. With the estimate $\epsilon \sim \frac{U^3}{L}$ they can be written as

$$\eta = \left(\frac{\nu^3 L}{U^3}\right)^{1/4} \tag{3.13}$$

$$\tau_\eta = \left(\frac{\nu L}{U^3}\right) \tag{3.14}$$

Both these scales are coupled by the Reynolds number:

$$\frac{L}{\eta} = Re^{3/4} \tag{3.15}$$

$$\frac{\tau_{\mathrm{L}}}{\tau_\eta} = {Re_{\mathrm{L}}}^{1/2} \tag{3.16}$$

It can be seen from these to equations that the difference between the scales increases for higher Reynolds numbers.
A scale between these two is the Taylor microscale, often referred to as 'turbulence length scale'. Although it lacks of a physical interpretation, it is often used to describe the intermediate range between integral and Kolmogorov scales. Its definition is:

$$\lambda = \sqrt{15\frac{\nu}{\epsilon}}|\boldsymbol{v'}| \tag{3.17}$$

with $|\boldsymbol{v'}|$ denoting the absolute value of the velocities fluctuation. This scale can be used to compute another Reynolds number $Re_\lambda$:

$$Re_\lambda = \frac{|\boldsymbol{v'}|\lambda}{\nu} \tag{3.18}$$

Together these scales form a powerful tool to understand and compute turbulent flows.

## 3.2 Particle dynamics

This work deals with particle laden fluids. Therefore the impact of them on the flow behavior of the fluid needs to be described. This phenomenon is called two-way-coupling and the exchanged energy per time between fluid and particles is called coupling rate.
Here small and heavy, rigid particles, with a spherical shape are considered. Their radius $r_p$ is even smaller than the Kolmogorov scale $\eta$, but also large enough to neglect the Brownian motion.
Due to the small particle concentration, the best and most common way to describe these flows is the point particle approach, which means that every particle is treated as an mathematical point source of mass, momentum and energy. In this case we focus on the momentum exchange.Effects like particle-particle interactions, particle-wall interactions are also neglected.
At describing the motion of the particles in the following the fact, that we deal with gas-solid flows is an advantage, since we can make several simplifications. First the perspective is taken on the influence of the particles on the carrier fluid. Here the assumptions, that the fluid is incompressible and the mass exchange over the particle surface is zero are used. Hence the continuity equation becomes:

$$\boldsymbol{\nabla} \cdot \boldsymbol{u}. \tag{3.19}$$

The Navier Stokes equation, described in chapter 1, becomes:

$$\rho\left(\frac{\partial \boldsymbol{u}}{\partial t} + \boldsymbol{\nabla} \cdot (\boldsymbol{u}\boldsymbol{u})\right) = -\boldsymbol{\nabla} p + \mu \nabla^2 \boldsymbol{u} - \boldsymbol{F}. \tag{3.20}$$

The influence of the particles on the fluid is represented by the new term $\boldsymbol{F}$, wich describes the force per unit volume on the fluid. $\boldsymbol{F}$ could be approximated by a superposition of Dirac's delta functions over all particles, centered at the location $x_p^n$ of each particle:

$$\boldsymbol{F} = \sum_{n=1}^{N_\mathrm{p}} \boldsymbol{f}^\mathrm{n}(\boldsymbol{x}_\mathrm{p}^\mathrm{n}) \delta(\boldsymbol{x} - \boldsymbol{x}_\mathrm{p}^\mathrm{n}). \tag{3.21}$$

$\boldsymbol{x}_\mathrm{p}^\mathrm{n}$ is the position of the n-th particle and results from the kinematic equation

$$\frac{\partial \boldsymbol{x}_\mathrm{p}}{\partial t} = \boldsymbol{v}_\mathrm{p}^\mathrm{n} \tag{3.22}$$

$\boldsymbol{v}_\mathrm{p}$ and is the velocity of the n-th particle. $\boldsymbol{f}^\mathrm{n}$ is the sum of forces acting between fluid an particles. The delta function becomes one if $\boldsymbol{x} - \boldsymbol{x}_\mathrm{p}^\mathrm{n}$ becomes zero. Otherwise its zero. In this way, the coupling forces act at the positions of the particles on the fluid. Also it plays also an important role in the equation of motion of the

particles:

$$\mathrm{v}\rho_\mathrm{p}\frac{\partial \boldsymbol{v}_\mathrm{p}^\mathrm{n}}{\partial t} = \mathrm{v}\rho_\mathrm{p}\boldsymbol{g} + \boldsymbol{f}^\mathrm{n}(\boldsymbol{x}_\mathrm{p}^\mathrm{n}) \tag{3.23}$$

As already mentioned $\boldsymbol{f}^\mathrm{n}(\boldsymbol{x}_\mathrm{p}^\mathrm{n})$ could be devided in several forces. Then the equation of particle motion looks like:

$$m_\mathrm{p}\frac{\partial \boldsymbol{v}_\mathrm{p}^\mathrm{n}}{\partial t} = m_\mathrm{p}\boldsymbol{g} + \rho\mathrm{v}\left(\frac{D\boldsymbol{u}}{Dt} - \boldsymbol{g}\right) + \boldsymbol{f}_\mathrm{d} + \boldsymbol{f}_\mathrm{l} + \boldsymbol{f}_\mathrm{a} + \boldsymbol{f}_\mathrm{h} + \boldsymbol{f}_\mathrm{additional} \tag{3.24}$$

Here $\boldsymbol{f}_\mathrm{d}$ represents the hydrodynamical drag force that is parallel to the undisturbed streamlines, which depends on an empirical drag coefficient $C_\mathrm{d}$:

$$\boldsymbol{f}_\mathrm{d} = -\frac{3}{4}\rho\mathrm{v}\frac{C_\mathrm{d}}{d}|\boldsymbol{v}_\mathrm{p} - \boldsymbol{u}|(\boldsymbol{v}_\mathrm{p} - \boldsymbol{u}) \tag{3.25}$$

It depends on the empirical drag coefficient defined after Schiller and Naumann as

$$C_\mathrm{d} = \frac{24}{Re_\mathrm{p}}(1 + 0.15Re_\mathrm{p}^{0.687}). \tag{3.26}$$

$\boldsymbol{u}$ is the velocity of the uniform stream, which is enough away from the particle that it is undisturbed from the particle. The other partial hydrodynamical force, the lift force $\boldsymbol{f}_\mathrm{l}$ is perpendicular to the undisturbed streamlines. Furthermore the added mass force $\boldsymbol{f}_\mathrm{a}$ represents the influence of the inertia of the fluid that has an impact on the particle, if it has a different acceleration than the mean flow. Hence it could be determined by:

$$\boldsymbol{f}_\mathrm{a} = \frac{1}{2}\rho\mathrm{v}\left(\frac{D\boldsymbol{u}}{Dt} - \frac{d\boldsymbol{v}_\mathrm{p}}{dt}\right) \tag{3.27}$$

The history force $\boldsymbol{f}_\mathrm{h}$ takes diffusion and convection, that results out of the vortices behind the particles, into account. Basselt's result, neglecting the finite size correction, is proportional to $\boldsymbol{\nabla}^2\boldsymbol{u}$:

$$\boldsymbol{f}_\mathrm{h} = \frac{3}{2}d^2\rho\sqrt{\pi\nu}\int_{t_0}^{t}\frac{\mathrm{d}t'}{(t-t')^{1/2}}\left(\frac{\mathrm{D}\boldsymbol{u}}{\mathrm{D}t'} - \frac{\mathrm{d}\boldsymbol{v}_\mathrm{p}}{\mathrm{d}t'}\right) \tag{3.28}$$

The last term $\boldsymbol{f}_\mathrm{additional}$ is attached for the case that we have to take other forces like electrostatic interactions into account. In this case of gas-solid suspensions there could be made several simplifications. In the following there is shown with an rough approximation that the added mass and history forces are negligible compared with the drag force. We use the approach that the relative velocity is of the same order as the terminal velocity $v_\mathrm{t}$. The terminal velocity is the velocity of a particle in a resting fluid, when gravitation and drag force are in equilibrium. Then if the added mass and the drag force are compared, we get the following equation:

$$\frac{|\boldsymbol{f}_\mathrm{a}|}{|\boldsymbol{f}_\mathrm{d}} \simeq \frac{\frac{1}{2}\rho\mathrm{v}g}{\frac{3}{4}\rho\mathrm{v}(C_\mathrm{d}/d)v_\mathrm{t}^2}\frac{a_\mathrm{r}}{g} = \frac{1}{2}\frac{\rho}{\rho_\mathrm{p}}\frac{a_\mathrm{r}}{g} \tag{3.29}$$

with

$$a_{\mathrm{r}} = (\frac{\mathrm{D}\boldsymbol{u}}{\mathrm{d}t} - \frac{\mathrm{d}\boldsymbol{v}_{\mathrm{p}}}{\mathrm{d}t}) \tag{3.30}$$

Since in gas-solid suspensions the particle density is of an factor of 1000 higher than the fluid density, it shows that, if it's not the unlikely case that the relative acceleration is of the same order higher than the gravity, the added mass force is negligible compared to the drag force. The relation of the history force and the added mass force with the assumption of comparable accelerations, with the relexation time of the order of $\tau$ results in

$$\frac{|\boldsymbol{f}_{\mathrm{h}}|}{|\boldsymbol{f}_{\mathrm{a}}|} \simeq 18\sqrt{\frac{\nu\tau}{d^2}}. \tag{3.31}$$

Hence it is of the order of the ratio of the diffusion length to the particle diameter, which might be of the order of one, if $\tau \sim \frac{d^2}{\nu}$. Hence the history force is also negligible compared to the drag force. For the lift force the situation is the same, because is is also proportional to the fluid density and the length scale of the ambient flow vorticity might be much greater than the particle size. It shows that the particle motion is only depending on the the hydrodynamical drag force which results from the actual difference between the fluid velocity $\boldsymbol{u}(\boldsymbol{x}_{\mathrm{p}})$ at particle position $\boldsymbol{x_p}$ and the particle velocity $\boldsymbol{v_p}$. Due to this asumptions equation (3.17) becomes

$$\rho_{\mathrm{p}} \frac{d{\boldsymbol{v}_{\mathbf{p}}}^{\mathrm{n}}}{dt} = \rho_{\mathrm{p}}\boldsymbol{g} + \boldsymbol{f}_{\mathrm{d}}^{\mathrm{n}} \tag{3.32}$$

This equation can be rewritten with help of the relaxation time $\tau_{\mathrm{p}}$, which physically represents the time scale over which the drag force decreases the particle relative veloctity to zero. At one point in the fluid with the proportionality

$$\frac{\rho_{\mathrm{p}} v_{\mathrm{p}}}{\tau_{\mathrm{p}}^{\mathrm{n}}} \sim f_{\mathrm{d}} \tag{3.33}$$

it follows the equation for the releaxation time

$$\tau_{\mathrm{p}}^{\mathrm{n}} = \frac{4}{3}\frac{\rho_{\mathrm{p}}}{\rho}\frac{d}{C_{\mathrm{d}}^{\mathrm{n}}}\frac{1}{v_{\mathrm{r}}^{\mathrm{n}}} \tag{3.34}$$

where $v_{\mathrm{r}}^{\mathrm{n}}$ is the relative velocity. With equation (3.26) and the Reynoldsnumber in relation to the particles $Re_{\mathrm{p}}^{\mathrm{n}} = \frac{v_{\mathrm{r}}^{\mathrm{n}} d}{\nu}$, with the particle diameter d it follows

$$\tau_{\mathrm{p}}^{\mathrm{n}} = \frac{\rho_{\mathrm{p}}}{p}\frac{d^2}{18\nu}\frac{1}{1 + 0.15 Re_{\mathrm{p}}^{\mathrm{n}\,0.687}}. \tag{3.35}$$

Then the equation of motion of the particles becomes

$$\rho_{\mathrm{p}} \frac{d\boldsymbol{v}^{\mathrm{n}}}{dt} = \rho_{\mathrm{p}}\boldsymbol{g} - \rho_{\mathrm{p}}\frac{\boldsymbol{v}_{\mathrm{p}}^{\mathrm{n}} - \boldsymbol{u}^{\mathrm{n}}}{\tau_{\mathrm{p}}^{\mathrm{n}}}. \tag{3.36}$$

Using the Stokes response time $\tau_{\mathrm{ps}} = \frac{\rho_{\mathrm{p}} d^2}{18\nu\rho}$, that is the particle response time at resting fluid condtions, there finaly exists another form of this equaion

$$\rho_{\mathrm{p}} \frac{d\boldsymbol{v}_{\mathrm{p}}^{\mathrm{n}}}{dt} = \rho_{\mathrm{p}} \boldsymbol{g} - \rho_{\mathrm{p}} \frac{\boldsymbol{v}_{\mathrm{p}}^{\mathrm{n}} - \boldsymbol{u}^{\mathrm{n}}}{\tau_{\mathrm{ps}}} f_{\mathrm{d}} \tag{3.37}$$

with $f_{\mathrm{d}} = 1 + 0.15 Re_{\mathrm{p}}^{\mathrm{n}\,0.687}$, which is not the drag force.

The coupling rate $\psi$, that describes the transfered Energy per time between particles and fluid, is defined as

$$\psi = \boldsymbol{F}\boldsymbol{u}. \tag{3.38}$$

Hence it results from the force per unit volume exerted between the fluid and the particles and the main velocity of the fluid. It is an useful variable to describe, how much the main fluid and the particles influence each other.

# 4 Numerical methods

To simulate flows like those described above we have two options. The direct numerical simulation (DNS) is the easier one to understand, although it is numerically very expensive. The Large-eddy simulation (LES) is numerically more capable, still we must accept certain inaccuracies. These two numerical methods are now discussed in the following chapter.

## 4.1 Direct numerical simulation

The basis of the direct numerical simulation (DNS) are the Navier-Stokes equations as described above. The idea is that the computer is very good at calculating and solves these equations completely. This provides a very accurate result, as all scales of motion are being resolved. Still it requires an immense level of comptational resources which increases rapidly with the Reynolds number. These computational resources were not available until the 1970s. Even though it is not advisable to resolve every scale of motion, if only the contained energy is of greatest interest. With the large-eddy simulation, as described below, the comptational effort is 99.98 % less compared to DNS, which indeed is the fraction of the dissipative scale. This leaves 0.02 % of the flow, which is correlative with the fraction of the energy-containing larger-scale [**?**].

## 4.2 Large-eddy simulation

Due to the fact that DNS is effortful and wasting resources if a fully resolved resolution is not required, large-eddy simulation (LES) was created to save time and resources. This is especially efficient if mainly the temproal energy trend is considered, because the energy containing larger-scale motion is completely resolved and the indeed small effects of the expensive smaller-scale motion are just modelled. Otherwise in DNS resolving the small dissipative scale would require most of the computational resources.
Simulating only the larger-scale motions is also called filtering, which means that the smaller-scale motions are filtered out. To model the filtered smaller-scale motions ususally a subgrid-scale (SGS) model is used. According to Hickel (2007) the interference between explicit SGS and the trunctation error can be exploited, i.e. the trunctation error can serve as model of the effects of unresolved scales, which is therefore an implicit SGS model. Thus we call it implicit LES (ILES) [**?**].

## 4.3 Discretisation

To integrate the Lagrangian particle tracking equations, discussed above, a predictor-corrector scheme based on the trapezoidal rule for numerical integration

$$f(t+\delta t) \approx f(t) + \frac{\delta t}{2}\left[\frac{\partial f(t)}{\partial t} + \frac{\partial f(t+\delta t)}{\partial t}\right] \tag{4.1}$$

is used.
The first step is the prediction of the new particle position $\boldsymbol{x}_{n+1}^{(\mathrm{p})}$ using a Taylor expansion for a small time step $\delta t$

$$\boldsymbol{x}_{n+1}^{(\mathrm{p})} = \boldsymbol{x}_n + \delta t \boldsymbol{v}_n + \frac{1}{2}\delta t^2 \boldsymbol{a}_n. \tag{4.2}$$

Due to the computational effort we will put $\boldsymbol{u}_{n+1}^{(\mathrm{p})}$ on the level of the nearest cell fluid velocity.
The updated velocity and acceleration are calculated as

$$\boldsymbol{v}_{n+1} = \frac{\boldsymbol{v}_n + \frac{1}{2}\delta t\left(\boldsymbol{a}_n + \frac{f_\mathrm{D}}{\tau_\mathrm{p}}\boldsymbol{u}_{n+1}^{(\mathrm{p})} + \boldsymbol{g}\right)}{1 + \frac{1}{2}\frac{f_\mathrm{D}}{\tau_\mathrm{p}}\delta t}, \tag{4.3}$$

$$\boldsymbol{a}_{n+1} = \frac{\frac{f_\mathrm{D}}{\tau_\mathrm{p}}\left(\boldsymbol{u}_{n+1}^{(\mathrm{p})} - \boldsymbol{v}_n - \frac{1}{2}\delta t \boldsymbol{a}_n\right) + \boldsymbol{g}}{1 + \frac{1}{2}\frac{f_\mathrm{D}}{\tau_\mathrm{p}}\delta t}. \tag{4.4}$$

The updated particle position must be corrected by an additional term according to the trapezoidal rule

$$\boldsymbol{x}_{n+1} = \boldsymbol{x}_n + \frac{1}{2}\delta t\left(\boldsymbol{v}_{n+1} + \boldsymbol{v}_n\right) + \frac{1}{12}\delta t^2\left(\boldsymbol{a}_{n+1} - \boldsymbol{a}_n\right). \tag{4.5}$$

## 4.4 Particle clustering

The high number of point particles require even more computational resources for the particle-laden simulation. The main idea to reduce this requirement is to create clusters of point particles, meaning that a new variable $m_\mathrm{c}$ is introduced. We consider a cluster of $m_\mathrm{c}$ point particles as one larger point particle, i.e. the program has less particles to simulate. To compensate this lack of particles, the coupling force is multiplied by $m_\mathrm{c}$, due to the $m_\mathrm{c}$-fold mass of the (cluster-)particles. In chapter 5 (results) we evaluate the legitimacy of particle clustering and the maximum acceptable value of $m_\mathrm{c}$.

Projektion (noComputationalParticles), Diskretisierung implizite LES (Motivation fuer LES - Pope Chapter 9, Bild 9.4), DNS

# 5 Results

The simulations where carried out using ZFS, the simulation tool developed and implemented at the Institute of Aerodynamics at RWTH Aachen University [**?**] [**?**]. The tool is capable of simulating finite-volume flows of compressible fluids. In this case the turbulence was simulated on a cubic grid using $64^3$,$96^3$,$128^3$ and $256^3$. The first three cases where simulated using LES, the case in which $256^3$ cells where used is carried out as DNS. Futher information can be gained by looking at [**?**, p.344-357 for DNS and p. 558-639 for LES].

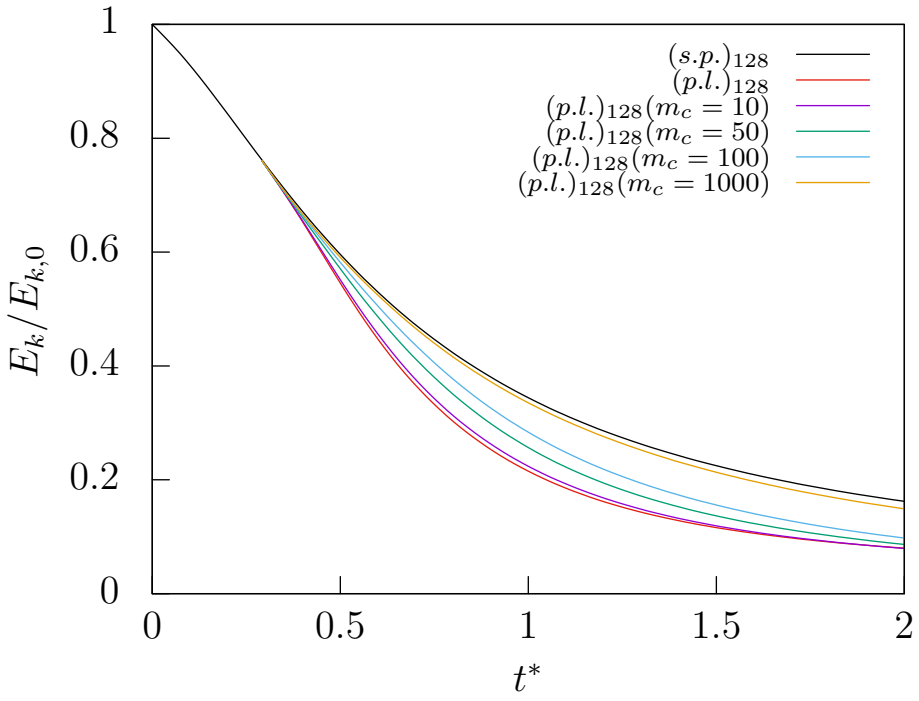


Figure 1: Kinetic Energy over eddy turnover times for different numbers of particles

For simplification, the special case of isotropic turbulence was used. For this idealised flow form the statistical velocities are invariant in all directions of the grid. It follows that the flows velocity are invariant for rotations and reflections. The turbulence was initialised using a seed-based random generator. To achieve physical results, the simulation of the particle-free flow was carried out to timestep 150, at which a restart file was written out. This procedure ensures a fully developed turbulent flow, whom has emancipated from the initialisation. In this flow field, a specific number of spherical particles were injected.

As noted in [**?**], particles tend to cluster in certain regions of the turbulent flow. This behavior can bee used to minimize computational effort for simulating the

flow while still achieving high quality results. To investigate the differences in accuracy for different sizes of particles sizes, the variable $m_c$ was introduced to the code describing the number of particles in one cluster. The simulations where then set up with the overall same number of particles ($10^6$), just the number of particles in one cluster was altered. Then the simulations where carried out normally and result in the following graphs (Figure 1, 2 and 3). It can be seen in figure 1 that the decay in kinetic energy from the starting point depends highly on the number of clustered particles. **With 10 particles per cluster, the solutions could be usable to get a first impression for technical purposes, all other simulations show a very high variety.**

Fitting to this first results, the Graphs of figure 2 and 3 clearly show that for sim-

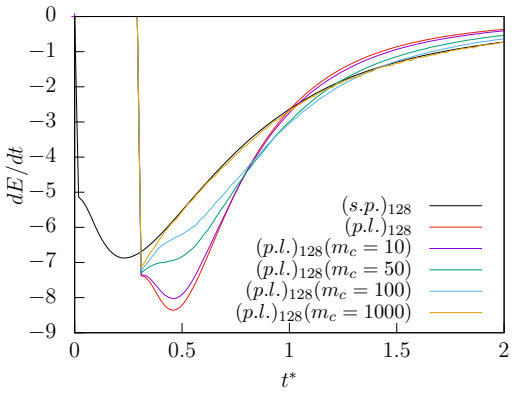


Figure 2: Change in kinetic Energy over eddy turnover times

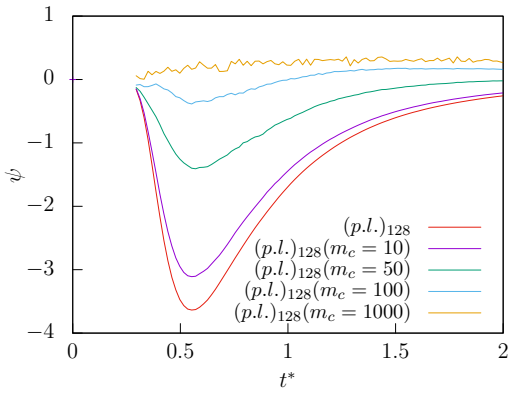


Figure 3: Coupling Rate over eddy turnover times

ulations with highly clustered particles the simulations results differ a lot. Looking at the results for the change in kinetic Energy, the difference becomes evident: The lower $m_c$ is, the higher is the drop in kinetic Energy. This behavior can be seen because of the particles initially 'soaking up' energy, then in later phases of the flow giving it back in form of their inertia and speed, which they gathered in the beginning. **This effect should grow bigger by particle size and weight.** This change in energy transfer occurs at the unclustered simulation at about one eddy turnover time. In cases with more clustered particles it occurs later, only the case in which 1000 particles where clustered shows a strange behavior. It catches up the particle-free case very fast, which leads to the conclusion that the amount of clusters is so small that the flow almost behaves like one without particles. Additional the change in kinetic Energy shows inconstancy which can also be traced back to the small cluster number. The amount is just to small to achieve high-quality information in the statistical variables.

The same impression can be achieved by looking at the graphs describing the coupling rate. The particle-laden-case makes the biggest jump into negative coupling rate. The higher the amount of coupled particles, the lower is the negative coupling rate. This evolution continues until the physicality vanishes and the randomness starts to show at the results for $m_c$ higher than 50.
Being very similar in the time shortly after the injection, the flow statistics diverge more and more when time passes by. The variables of these simulations one turnover time after the injection can be found in table 1 on page 17. The ratio of the densities for this simulations was set to $\frac{\rho_p}{\rho} = 1000$. At the timestep of injection the particle response time $\tau_p = \frac{d^2}{18\nu}\frac{\rho_p}{\rho}$ was 0.03497 **Uebepruefen, ist die Viskositaet die richtige? Diameter einfuegen, Tabelle ueberarbeiten**.

| $m_c$ | $u_0$ | $\epsilon$ | $\lambda$ | $\eta$ | $Re_\lambda$ |
|---|---|---|---|---|---|
| 1 | 0.21496 | 0.79150 | 0.0432 | 0.00333 | 43.360 |
| 10 | 0.22364 | 1.02918 | 0.03866 | 0.00312 | 39.5653 |
| 50 | 0.25654 | 1.78788 | 0.03144 | 0.00272 | 34.4702 |
| 100 | 0.28357 | 2.26144 | 0.02940 | 0.00257 | 33.8869 |
| 1000 | 0.33543 | 2.2855 | 0.03184 | 0.00256 | 39.8993 |

Table 1: Variables of the first set of simulations **about** one turnover time after injection for the $128^3$-case

To find out at which number of particles the results are sufficiently exact, a second set of simulations was carried out. As mathematics of turbulent flows are based on averaged variables, small numbers of particles can lead to false and even unphysical results. In these simulations, no particle clustering was used, just different amount of particles were injected into the same flow. For these simulations similar properties to the ones from the first set of simulations were used, just the mentioned number of particles was changed. The results can be seen on page 18 on figure 4. The normalized difference in **kinetic Energy** shows in this one-time simulation a clear correlation between particle number and accuracy in the simulation. Athough this was just a single initialization of particles in a flow, it can be stated that simulations using only $10^2$, $10^3$ or even up to $10^4$ particles are not accurate enough for technical or scientific use of the data. One-time simulations in other gridsizes show similar results.

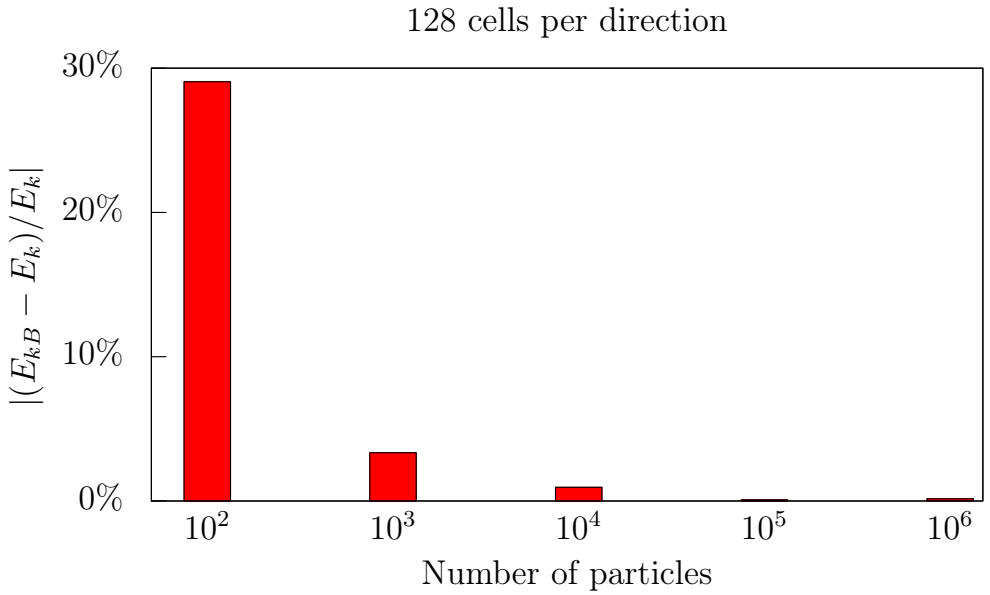


Figure 4: Results for initializing different numbers of particles

## 6 Conclusion and outlook

Offene Themen: Statistische Auswertung der Anzahl der Partikel (Konvergenz)

**Acknowledgements**

# 7 References